

Study on elastic-plastic behaviour of inclusions in cold drawn wire by using reverse analysis and nanoindentation test

Kyung-Hun Lee¹, Jung-Min Lee², Se-In Ji³, Jae-Hong Kim³, Dae-Cheol Ko⁴, and Byung-Min Kim^{3,a}

¹ PNU-IFAM JRC, Pusan National University, Geumjeong-gu, Busan, Korea

² Dongnam Regional Division, Korea Institute of Industrial Technology, Gangseo-gu, Busan, Korea

³ School of Mechanical Engineering, Pusan National University, Geumjeong-gu, Busan, Korea

⁴ ERC/ITAF, Pusan National University, Geumjeong-gu, Busan, Korea

Abstract. The purpose of this study is to investigate the elastic-plastic behavior of inclusions, i.e. SiO₂ particles, in cold drawn wire using reverse analysis and nanoindentation test. First, the nanoindentation tests were performed to obtain indentation load P – penetration depth h curves. Second, the reverse analysis which is consisted of various dimensionless functions including change in E^*/σ_r , W_p/W_t and n was used to extract the elastic-plastic properties of the indented inclusions and metals from indentation responses. To verify the accuracy of calculated properties, uniaxial tensile tests were performed for different materials which are AISI 1045 and AISI 1080. Results (E , σ_y , n) of tensile tests for each material were also compared with those of nanoindentation tests.

1. Introduction

Nanoindentation test is an efficient method for measuring the mechanical properties of material such as the elastic modulus and hardness using the indentation load – penetration depth curve. Technological advances of numerical and theoretical analysis have recently allowed us to extract the elastic-plastic properties for not only bulk materials but also thin films or coated metal.

The basic relationship between the elastic-plastic behaviour of metal can be generally identified by dimensional analysis [1–3]. Especially, Lee et al. [3] performed a parametric study of 138 cases with various elastic-plastic parameters using FE analysis of indentation. They proposed a set of dimensionless functions that can investigate the elastic-plastic properties from the indentation response.

This study is designed to calculate mechanical properties of inclusions, i.e. SiO₂ particles, in cold drawn wire by using reverse analysis proposed by Lee et al. [3]. The reverse analysis which is consisted of various dimensionless functions including change in C , E^*/σ_r , and W_p/W_t can be extract the elastic-plastic properties of indented materials, such as E , σ_y and n . The validity of calculated mechanical properties was verified to nanoindentation and tensile tests.

^a Corresponding author: bmkim@pusan.ac.kr

2. Reverse analysis

General $P-h$ curve of the elastic-plastic materials is shown in Fig. 1. In previous studies [2, 3], a loading curve in $P-h$ curve is described by Kick's law.

$$P = Ch^2 \quad (1)$$

where P , h and C are the indentation load, depth and loading curvature, respectively. An unloading curve can be also expressed as an initial unloading slope dP_u/dh_{hm} . The term of $W_t (= W_e + W_p)$ is the total work performed during whole indentation process. W_e and W_p represent the elastic work during unload process and the plastic work, respectively.

In order to determine the mechanical properties of the inclusions in cold drawn wire, the reverse analysis was performed as described in Ref. [3] and its detailed procedure is shown in Fig. 2. First, the reduced modulus E^* is calculated by using Π_2 function and substituting the C and W_p/W_t obtained from the $P-h$ curve. Second, the representative stress σ_r is obtained by using Π_1 function and substituting the C and E^* . Third, the representative strain ε_r is determined by substituting E^* and σ_r into Eq. (6). Fourth, the hardness H of the indented material is calculated by using Π_4 function and substituting E^* and W_p/W_t . Fifth, the strain hardening exponent n is confirmed by Π_3 function and substituting C , H and E^*/σ_r . Finally, the initial yield stress σ_y is obtained by substituting E^* , σ_r , ε_r and n into Eq. (7).

$$\begin{aligned} \frac{C}{\sigma_r} = \Pi_1 \left(\frac{E^*}{\sigma_r} \right) = & 0.00656 \left[\ln \left(\frac{E^*}{\sigma_r} \right)^3 \right] - 0.17093 \left[\ln \left(\frac{E^*}{\sigma_r} \right)^2 \right] \\ & + 1.47864 \left[\ln \left(\frac{E^*}{\sigma_r} \right) \right] + 0.42932 \end{aligned} \quad (2)$$

$$\frac{C}{E^*} = \Pi_2 \left(\frac{W_p}{W_t} \right) = 2.107 - 2.1092 \left(\frac{W_p}{W_t} \right) \quad (3)$$

$$\begin{aligned} \frac{C}{H} = \Pi_3 \left(\frac{E^*}{\sigma_r}, n \right) = & (0.00802n^3 - 0.02194n^2 + 0.00677n + 0.00858) \left[\ln \left(\frac{E^*}{\sigma_r} \right)^3 \right] \\ & + (0.11401n^3 + 0.17866n^2 - 0.0163n - 0.20838) \left[\ln \left(\frac{E^*}{\sigma_r} \right)^2 \right] \\ & + (-1.06707n^3 - 0.57297n^2 - 0.56114n + 1.68803) \left[\ln \left(\frac{E^*}{\sigma_r} \right) \right] \\ & + (0.97574n^3 + 1.20917n^2 + 0.02855n + 0.09175) \end{aligned} \quad (4)$$

$$\frac{H}{E^*} = \Pi_4 \left(\frac{W_p}{W_t} \right) = 0.244 - 0.245 \left(\frac{W_p}{W_t} \right)^{0.78908} \quad (5)$$

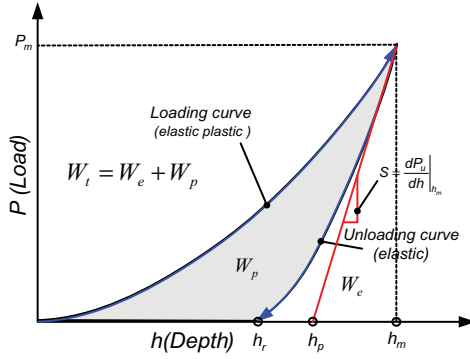


Figure 1. Typical load – penetration depth curve during indentation test with elastic-plastic deformation.

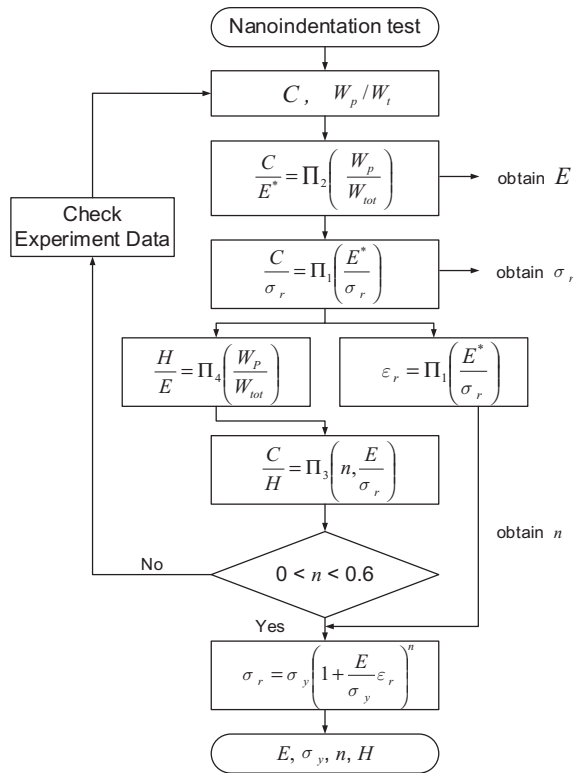


Figure 2. Reverse algorithm for extract elastic-plastic properties of indented materials. [3].

$$\varepsilon_r = \exp\left(-3.91 + \frac{166.7}{E^*/\sigma_r + 177.3}\right) \quad (6)$$

$$\sigma_r = \sigma_y \left(1 + \frac{E}{\sigma_y} \varepsilon_r\right)^n \quad (7)$$

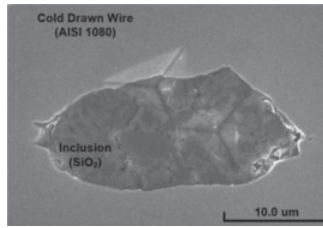


Figure 3. SEM image at indented material (AISI 1080 & SiO₂ inclusion).

Table 1. Results of uniaxial tensile tests.

Material	$E(\text{MPa})$	σ_y	n
AISI 1045	210.3	337.1	0.191
AISI 1080	214.7	688.9	0.206

Table 2. Comparisons E^*/σ_r , σ_r and ϵ_r calculated from Dao's and current reverse analysis.

Materials	Dao's reverse analysis		Current reverse analysis		
	E^*/σ_r	σ_r ($\epsilon_r = 0.033$)	E^*/σ_r	σ_r	ϵ_r
AISI 1045	368.67	515.13	376.83	493.37	0.0271
AISI 1080	566.46	765.32	100.01	1850.00	0.0201
Inclusion (SiO ₂)	381.18	190.91	95.12	1178.31	0.0370

Table 3. Comparisons of Dao's and current reverse analysis.

Material	Indentation test			Dao's reverse analysis			Current reverse analysis		
	C (GPa)	W_p/W_t	dP_u/dh	E (GPa)	σ_y (MPa)	n	E (GPa)	σ_y (MPa)	n
AISI 1045	59.32	0.923	1.218	217.53	242.85	0.308	200.03	346.11	0.211
AISI 1080	71.76	0.908	1.054	192.55	763.10	0.195	205.62	631.61	0.350
Inclusion (SiO ₂)	98.44	0.775	0.846	211.67	186.38	0.651	113.83	164.85	0.550

3. Nanoindentation and tensile tests

To verify the effectiveness of the reverse analysis, both nanoindentation and tensile tests were performed for different materials which are AISI 1045 and AISI 1080. Only nanoindentation test were carried out to measure mechanical properties of inclusions which is a SiO₂, as shown in Fig. 3. Indentation specimens were indented on a commercial Nanoindenter XP of MTS with the Berkovich diamond indenter until the indentation load of 100 ~ 500 mN at a target strain rate of approximately 0.05. Nanoindentation tests were repeatedly conducted by five times per each material. For each materials, test results are shown in Tables 1–3. The results revealed that computational properties are well agreed with experimental values within $\pm 5\%$ and $\pm 9\%$ on E and σ_y , respectively.

4. Conclusion

Mechanical properties of SiO₂ particles in cold drawn wire were calculated by using the reverse analysis and nanoindentation test. The reverse algorithm consists of various dimensionless functions including change in E^*/σ_r , W_p/W_t and n . To verify the accuracy of calculated properties (E , σ_y and n), uniaxial tensile tests were performed for different materials which are AISI 1045 and AISI 1080.

This work was supported by the National Research Foundation of Korea (NRF) grant funded by the Korea government (MSIP) (No. 2012R1A5A1048294) and PNU-IFAM Joint Research Center.

References

- [1] Y.T. Cheng, C.M. Cheng, *Mat. Sci. Eng. R* **44**, 91–149 (2004)
- [2] M. Dao, N. Chollacoop, K.J. Van Vleet, T.A. Venkatesh, S. Suresh, *Acta Mater.* **49**, 3899–3918 (2001)
- [3] J.M. Lee, C.J. Lee, B.M. Kim, *Mat. & Des.* **30**, 3395–3404 (2009)